

e-ISSN: 2355-6544

Received: 05 April 2025; Revised: 12 May 2025; Accepted: 18 May 2025;

Available Online: 31 October 2025; Published: 31 October 2025.

Keywords:

Coastal Erosion, Remote Sensing, Deep Learning, Influence Factors

*Corresponding author(s) email: giangnh@hueuni.edu.vn Original Research Open access



Deep Learning for Coastal Erosion Assessment: Case Study of Vietnam's Coastal Regions

HuuBang Tran¹, HongGiang Nguyen^{2*}

- 1. Institute of Architecture, Construction and Transportation, Thu Dau Mot University, Thủ Dầu Một City 5500, Vietnam.
- Institute of Testing and Quality Assurance in Education, Hue University, Hue City 49000, Viet

DOI: 10.14710/geoplanning.12.2.139-158

Abstract

Vietnam's coastal erosion has experienced a significant increase cause climate change and anthropogenic factors over the past decade. This study intends to analyze the trends of coastline erosion, identify the factors that drive it, and utilize deep learning algorithms to estimate the erosion risk in the future. The National Centre for Hydro-Meteorological Forecasting of Vietnam, Open Development Mekong, and Landsat 8 OLI/TIRS satellite pictures taken between the years 2016 and 2022 are the sources of data for the study, in the 52 erosion prone locations across Vietnam's coastlines. The significant environmental factors for the model are the height of tides, waves, storm intensity, soil porosity, high monsoon rainfall, sea level rise, temperature, and coastal geomorphology. A Pearson correlation analysis indicates the strongest correlation between storm intensity, wave height, temperature alongside a strong negative correlation of tidal height with rainfall and coastal slope. Accuracy of the forecast was performed with five models: Recurrent Neural Network (RNN), Long Short-Term Memory Network (LSTM), Bidirectional Long Short-Term Memory Network (BiLSTM), Bidirectional RNN (BiRNN), and Hybrid RNN_LSTM. Among the tested models, the Hybrid RNN_LSTM outperformed others, achieving R² and a correlation coefficient to gain 0.77 and 0.91, respectively, at the same time, the study emphasized monsoon winds, storms intensity, and tidal height as the most impactful parameters. These findings can form the basis for data-driven policy and management strategies to improve coastal resilience. Further research should consider anthropogenic activities and land use changes to expand scope and improve model accuracy in areas experiencing global erosion.

> Copyright © 2025 by Authors, Published by Universitas Diponegoro Publishing Group. This open access article is distributed under a Creative Commons Attribution 4.0 International license



Introduction 1.

Coastal erosion has emerged as a critical global threat, driven by both natural processes and human activities. Some natural effects are tides and storm waves, geological structure, meteorological phenomena, and seismology, in addition to wave actions, oceanic circulations, and climatic changes (Brocx & Semeniuk, 2009; Morton, 2003; Nichols et al., 2018). On the other hand, coastal erosion is exacerbated inflow activities like construction of recreational facilities, flowage barriers, restructuring and flood control channel dredging, tree harvesting in particular softwood stands, and coastal green space decline (Owens, 2020; Sahavacharin et al., 2022; Van Tho, 2019). Additionally, these effects are aggravated by global warming. Infrastructure along coastlines paired with depleting sediment supplies and increasing sea levels can deteriorate coastal erosion (FitzGerald et al., 2008; Gracia et al., 2018). Small Pacific Islands, like Vietnam is some of the numerous places around the world that have been impacted by the above phenomena. The effects of coastal erosion can cause many issues including

loss of land from agriculture and aquaculture putting livelihood of coastal inhabitants at risk. These challenges impede sustainable development, highlighting the need of an active coastal management policy.

Coastal erosion is a big problem in Vietnam and 17 percent of the population is affected by this problem (Nga et al., 2025; Nguyen et al., 2018). Some major regions, such as the Mekong Delta, the central coastal region, and the Red River Delta, are more at risk because of rising sea levels, storms, decrease in river sediment, tidal waves, and monsoon winds. Different studies have been conducted on the causes of coastal erosion and its impact on certain regions such as Vietnam and Southeast Asia. Dong et al. (2024), studied the impact of climate change on coastline erosion in Southeast Asia, pointing out several causative agents such as historical sea level changes, geological structures, sediment supply, wave movement, tides, storm surges, longshore transport of sediments, and anthropogenic activities. The research also outlined possible actions that can be taken to deal with erosion problems.

Thepsiriamnuay & Pumijumnong (2019) displayed the Simulator of Climate Change Risks and Adaptation Initiatives (SimCLIM) and its impact model, "CoastCLIM" were utilized to project changes in relative sea level across 18 provinces of Thailand from 1995 to 2100. The result of their findings forecasted sea levels rise with either solution 17.50 cm to 147.90 cm resulting to coastal retreat from 41.64m to 517.09m. Karlsrud et al. (2017) used MIKE21 SW and SWAN models, together with the GENESIS model for longshore sediment transport to forecast sea-level rise along Vietnam's East Coast. The result found that sea-level rose faster than 3 mm/year between 1993 and 2008 and that an all-time high was reached with about 20 cm overall during the last decades. In addition, Ca Mau's coast was identified as particularly vulnerable to subsidence/land loss. Hens et al. (2018) presented an overview of threats, i.e., flooding, salinization, shoreline changes and decline in mangroves and wetlands in the Asia-Pacific region due to coastal erosion impacts in Vietnam. The study proposed adaptation strategies to increase coastal resilience.

Yasuhara et al. (2016) displayed riverside and coastal erosion in Mekong Delta, Vietnam by breakpoint statistics and explained reduced sediment supply from upstream, dykes collapse, sea-level rise, intensifying typhoons as the main reasons of undercutting. Yaacob et al. (2018) deployed to evaluate the sedimentological and morphological Terengganu's coastal stretch between Dungun and Kemaman. The study pointed out that coarser sand deposits and steeper coastal slopes were characteristic of the region's eastern beaches, influencing coastal stability. Duc & Hieu (2017) assessed the impact of sea-level rise on sea-dike stability in coastal infrastructure of Hai Hau Vietnam due to sea-level rise. It was concluded that accelerated erosion, scouring and wave-induced soil loss on dike slopes may lead serious threat to a coastal infrastructure.

Veettil et al. (2021) examined the use of bio shields in conserving coastal mangroves ecosystems of Vietnam. The results highlighted that bio shields not only preserve shoreline long-term ecology but also yield additional ecosystem services for environment sustainability. Lin et al. (2021) identified natural and anthropogenic coastal erosion factors were delineated by case studies along the south-central coast line of Vietnam. The study particularly stressed the dangers that natural risks and socio-economic activities constitute for the stability of the coast in the process.

Based on previous studies, the nature of coastal erosion and its vulnerability are the result of interactions between complex environmental and anthropogenic factors. The need for integrated management becomes clear before the associated long-term impacts can be observed. Although many studies have been conducted on coastal erosion, a systematic review of how climate change and natural hazards interact with each other in relation to their combined impact on Vietnam's coastline is still lacking. The relationship between climate change-related events and their impacts, their influence on coastal erosion, implications for livelihoods, and how adaptation measures work, requires stronger evidence.

This study next gathers and analyzes existing data, classifies the existing coastal erosion in Vietnam, identifies main factors determining the extent of erosion, and applies deep learning models to predict erosion trends. Therefore, this study aims to analyze coastal erosion trends, identify the factors that drive them, and use

deep learning algorithms to estimate future erosion risks. In addition, this study also provides context-specific interventions to reduce risk. The results are very important for policymakers, local governments, developers and environmental researchers so they can implement proven data-driven strategies addressing the needs, capacities and resilience of coastal communities under acute or extreme environmental and social-ecological pressures.

2. Data and Methods

The study employs a range of deep learning models, including LSTM, BiLSTM, RNN, BiRNN, and Hybrid RNN-LSTM, to analyze and forecast coastal erosion patterns along Vietnam's shoreline. The principles and functionalities of these models are described in detail below, highlighting their suitability for coastal erosion prediction and comparative performance in forecasting accuracy.

2.1. LSTM

It is designed to manage sequential data by effectively capturing long-term dependencies (Lindemann et al., 2021; Xiang et al., 2020). An overview of its architecture is presented in Figure 1, and its detail is as follow (i) Input Layer: The model receives a sequence of input data as a sequence of data points $X = [x_1, x_2, ... x_t]$, where t is the sequence length. (ii) Forget Gate (f_t) : Decides what information from the previous time step should be discarded from the cell state C_{t-1} with formulation (see equation 1):

$$f_t = \sigma(W^f * x_t + U^f * h_{t-1}^L + b^f).....(Eq.1)$$

This is done by applying a sigmoid activation function (σ) to produce values between 0 and 1 (0 = forget, 1 = retain).

(iii) Input Gate (i_t) and Candidate State $(\tilde{\mathcal{C}}_t)$: Determines which values from the current input and the previous output should be stored in the cell state. The new information should be added to the cell state as the equation (2) and equation (3)

$$i_t = \sigma(W^i * x_t + U^i * h_{t-1}^L + b^i).....(Eq.2)$$

$$\tilde{C}_t = tanh(W^u * x_t + U^u * h_{t-1}^L + b^u).....(Eq.3)$$

(iv) Cell State (C_t) : This is the memory of the LSTM that can carry information across time steps. It gets updated by the input gate and forget gate. The equation (4) indicates to combines past knowledge $f_t \odot C_{t-1}$ and new information $i_t \odot \tilde{C}_t$.

$$C_t = i_t \odot \tilde{C}_t + f_t \odot C_{t-1}) \dots (Eq.4)$$

(v) Output Gate (o_t^L) and Hidden state (h_t^L) : Determines what the output of the current LSTM cell should be. Equation (5,6) are used the cell state and a sigmoid activation to compute the output, which is passed to the next LSTM cell or used as the model's prediction (h_t^L) .

$$o_t = \sigma(W^o * x_t + U^o * h_{t-1}^L + b^o).....(Eq.5)$$

$$h_t^L = o_t \odot \tanh(C_t)$$
).....(Eq.6)

(vi)Fully Connected (Dense) Layer: Converts LSTM output into a final prediction in equation (7)

$$o_t^L = tanh(W^o * h_t^L + b^o)...(Eq.7)$$

The optimal component model features an input layer with 52 nodes, a hidden layer comprising 84 nodes, and a single output node. The Adam optimizer is employed for stochastic gradient descent, while Mean Squared Error (MSE) serves as the performance evaluation metric. The model is trained 150 epochs with a batch size of 12, and tanh (activation function) for tested in the hidden layer.

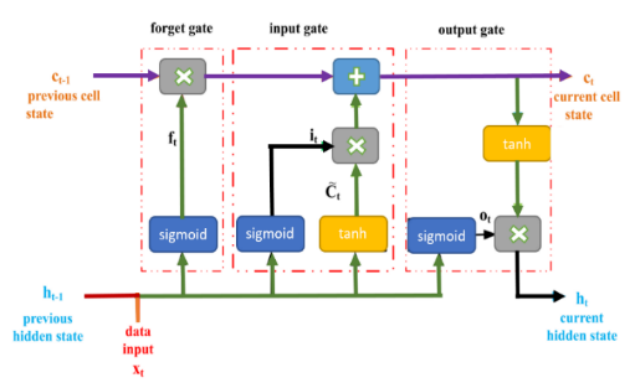


Figure 1. The LSTM Model's Working Structure

2.2. BiLSTM

BiLSTM model is an extension of the LSTM network, and Figure 2 shows a process of input sequences in both forward and backward directions (Hameed & Garcia-Zapirain, 2020; Siami-Namini et al., 2019). At each time, step t, a working method of two hidden states are indicated as below: (i) Forward hidden state $\overrightarrow{h_t^{BL}}$ calculated using equation (8):

$$\overline{h_t^{BL}} = \overline{o_t^{BL}} \odot \overline{\tanh(C_t)}....(Eq.8)$$

(ii) Backward hidden state $\overleftarrow{h_t^{BL}}$ calculated in reverse order in accordance with equation (9).

$$\overline{h_t^{BL}} = \overline{o_t^{BL}} \odot \overline{\tanh(C_t)}....(Eq.9)$$

(iii) The final hidden state is occupied by **concatenating** both forward and backward states in equation (10):

$$h_t^{BL} = [\overline{h_t^{BL}}, \overleftarrow{h_t^{BL}}] \dots (Eq.10)$$

(iv) Fully Connected (Dense) Layer; the concatenated hidden state h_t is passed through a **dense layer** for transformation. Output equation (11) presents:

$$o_t^{BL} = tanh(W^o * h_t^{BL} + b^o) \dots (Eq.11)$$

The optimal component model features are same LSTM model.

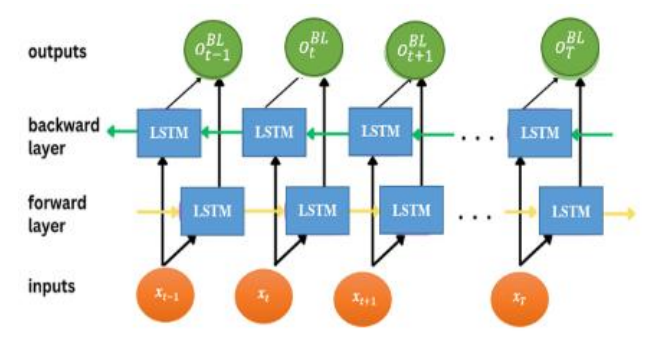


Figure 2. The BiLSTM Model's Working Structure

2.3. RNN

RNN model is architected for sequential data. It maintains a hidden state that captures information from previous time steps (Ming et al., 2017; Weerakody et al., 2021) (detail see Figure 3). Following is a detailed analysis of its structure. (i) Input Layer: The model receives a sequence of the input consists of sequential data, defined as $X = [x_1, x_2, ... x_t]$, where t is the sequence length; (ii) Hidden State Update (h_t^R). The equation (12) describes hidden state update:

$$h_t^R = tanh(W * x_t + U * h_{t-1}^R + b)$$
(Eq.12)

where, h_t^R , h_{t-1}^R , x_t , U, W, b are hidden state at time t, hidden state from the previous time step, input at time t, weight matrices, and bias term, respectively. The hidden state h_t^R acts as the network memory, and allowing information to be conducted across multiple time steps. (iii) Output Layer (σ_t^R), the final hidden state is passed through a fully connected (dense) layer to produce the desired output. Equation (13) presents the output at each time step.

$$o_t^R = tanh(W^o * h_t^R + b)$$
(Eq.13)

The optimal component model features are same LSTM model.

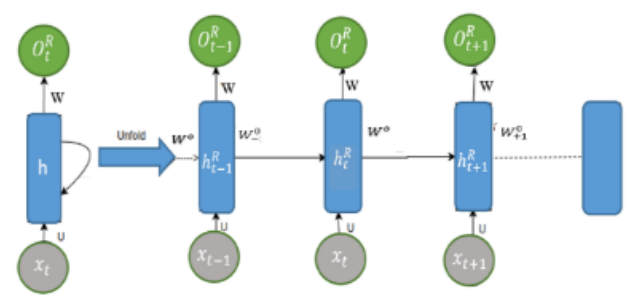


Figure 3. The RNN Model's Working Structure

2.4. BiRNN

BiRNN is an RNN expansion, Figure 4 describes a processes input sequences in both forward and backward directions (Li et al., 2019; Liu & Singh, 2016). At each time step t, an operating breakdown of two hidden states of BiRNN layer are described as below; (i) Forward hidden state $\overrightarrow{h_t^R}$: Calculated using equation (14):

$$\overrightarrow{h_t^R} = tanh(\overrightarrow{W} * x_t + \overrightarrow{U} * \overrightarrow{h_{t-1}^R} + \overrightarrow{b}) \dots (Eq.14)$$

(ii) Backward hidden state $\overleftarrow{h_t^R}$ calculated in reverse order in equation (15):

$$\overleftarrow{h_t^R} = tanh(\overleftarrow{W} * x_t + \overleftarrow{U} * \overleftarrow{h_{t-1}^R} + \overleftarrow{b}) \dots (Eq.15)$$

(iii) The final hidden state is occupied by concatenating both forward and backward states in equation (16):

$$h_t^R = [\overrightarrow{h_t^R}, \overleftarrow{h_t^R}]$$
(Eq.16)

(iv) Fully Connected (Dense) Layer: The concatenated hidden state h_t is passed through a dense layer for transformation. Output equation (17) presents:

$$o_t^R = tanh(W^o * h_t^R + b) \dots (Eq.17)$$

The optimal component model features are same LSTM model.

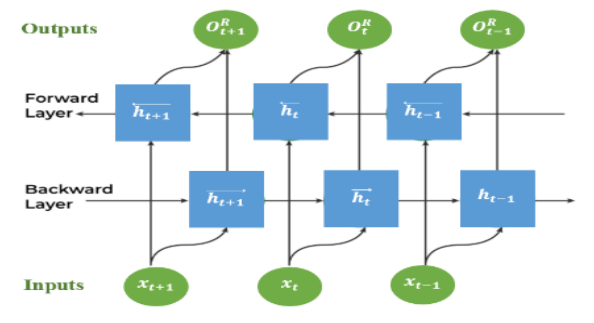


Figure 4. The BiRNN Model's Working Structure

2.5. Hybrid RNN-LSTM

The hybrid RNN-LSTM model (Figure 5) combines two types of RNN and LSTM (Al-Selwi et al., 2024; Donkol et al., 2023). This network is designed to process sequential data by learning dependencies and patterns across time. At the same time Figure 5 indicates the structural diagram for the model as (i) Input Layer: Processes and forwards input data to the model (see equation 18); (ii) RNN Layer: Handles sequence data and learns temporal patterns (see equation 19); (iii) LSTM Layer: Captures long-term dependencies in the data (see equation 20); (iv) Dropout Layers: Prevents overfitting by randomly ignoring certain neurons during training (see equation 21); (v) Dense (Output) Layer: Generates the final predictions based on learned features (see equation 22); (vi) Connections: Data flows sequentially through RNN, LSTM, and dense layers, with dropout layers enhancing generalization (see equation 23). In addition, the equations (18, 24) describe the working breakdown for the model.

The estimating sea erosion is as (see equation 24):

$$\widehat{est} = \sigma(W^o * h_t^H) \dots (Eq.24)$$

The model work such as input data is fed into the RNN layer, which captures temporal relationships in a lightweight manner. The processed information is passed to the LSTM layer, which learns both short-term and long-term dependencies in the sequence. The LSTM's output is regularized using the Dropout layer. Finally, the Dense layer generates predictions based on the processed sequence. The optimal component model features are same LSTM model; however, hidden layers for model include RNN hidden layer and LSTM hidden layer.

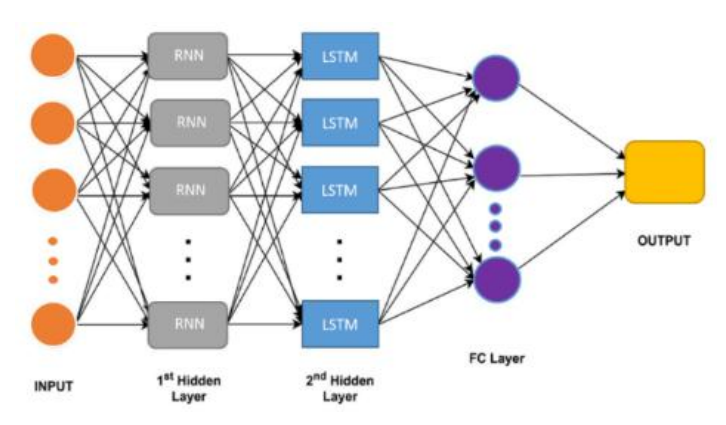


Figure 5. Hybrid RNN-LSTM Model's Structure

2.6. Metric of Accurate Parameters

Predicting accuracies depend on computing and comparing between the actual and predicted data. These metrics of the *accreting measured parameters* for the study such as the MAPE (Equation 25), RMSE (Equation 26), MAE (Equation 27), Squared (R²) (Equation 28), and CC (Equation 29). The indicators are shown as below (Kardani et al., 2020; Touzani et al., 2018):

$$MAPE(\%) = \frac{1}{n} \sum_{t=1}^{\left| \frac{x_t' - x_t \right|}{x_t}} \%. \qquad (Eq.25)$$

$$RMSE = \sqrt{\frac{\sum_{t=1}^{n} (x_t - x_t')^2}{n}} \qquad (Eq.26)$$

$$MAE = \frac{1}{n} \sum_{t=1}^{n} |x_t' - x_t| \qquad (Eq.27)$$

$$R_squared = 1 - \frac{\sum_{t=1}^{n} (x_t - x_t')^2}{\sum_{t=1}^{n} (x_t - \frac{1}{n} \sum_{t=1}^{n} x_t)^2} \qquad (Eq.28)$$

$$CC = \frac{\sum_{t=1}^{n} (x_t - \frac{1}{n} \sum_{t=1}^{n} x_t) \times (x_t' - \frac{1}{n} \sum_{t=1}^{n} x_t')}{\sqrt{\sum_{t=1}^{n} (x_t - \frac{1}{n} \sum_{t=1}^{n} x_t)^2 \times \sum_{t=1}^{n} (x_t' - \frac{1}{n} \sum_{t=1}^{n} x_t')^2}} \qquad (Eq.29)$$

where x_t , x_t' represent the estimated and actual values at time t, and n denotes the number of observed data points in the testing phase. The MEAN values of the predicted and actual data are represented by \bar{x} : \bar{x}' , respectively. The MAPE, RMSE, and MAE metrics approach zero for an ideal model (Kim & Kim, 2016; Niedbała, 2019), while R-squared (R²) can reach a maximum value of 1, indicating a highly accurate prediction (Brown, 2018; Gao, 2024; Karch, 2020; Salih & Abdulazeez, 2021).

Figure 6 demonstrates the workflow of the modeling experiment such as data preprocessing: The collected dataset undergoes statistical processing and is divided into training and testing sets. Model deployment: Five models are trained and evaluated to determine the most optimal indicators, performance evaluation: Key metrics such as RMSE, MAE, and R² are analyzed to identify the most effective forecasting model.

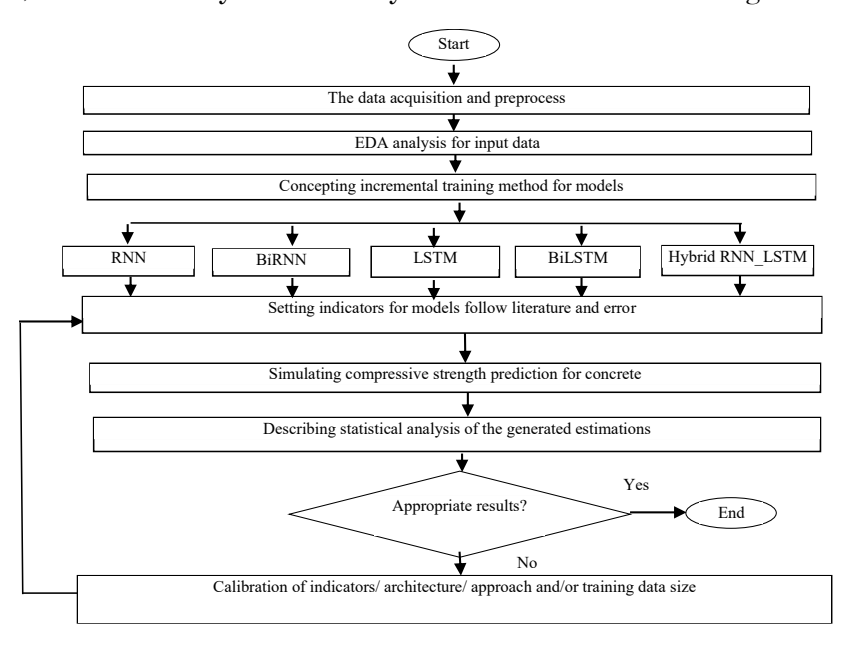


Figure 6. Workflow of the Study

3. Result and Discussion

Vietnam's coastline, located along the eastern edge of the Indochina Peninsula, plays a vital role in the country's history, culture, economy, and environment. Stretching approximately 3,260 km from Mong Cai in the north to Ha Tien in the south, it is associated with three major water bodies: the Gulf of Tonkin to the north, the south–central section of the East Sea, and the Gulf of Thailand to the southwest. This extensive coastline supports a wide range of activities, including aquaculture, fisheries, seaport operations, maritime trade, and renewable energy development.

However, coastal erosion has emerged as a severe challenge because of overexploited, the action of natural disasters and climate refresh. Most are in the Southwest and Central coastal provinces where river mouths as well as lowly forest cover protected areas. Minimal sediment supply leads to straight beaches or the nearly angulated beaches found along the interior coast and island coasts. They are typically also haphazardly populated which packages economic erosion effect. Figure 7-16 represents the spatial-temporal variability in shoreline erosion in significant coastal eroding areas of central coastal range and southwest coastal region during a five-year study period based on remote sensing data of each other. In which, Panel (a): Satellite imaged shows the specific places onshore that were target for coastal erosion. Panel (b): A digital elevation model (DEM) that shows topographical spatial changes occurring along the shorelines Panel (c)–(f) are one bands false-color composite satellite images in different years, where green stands for vegetation, yellow shows the land of transition land, and red reveals eroded or water places.

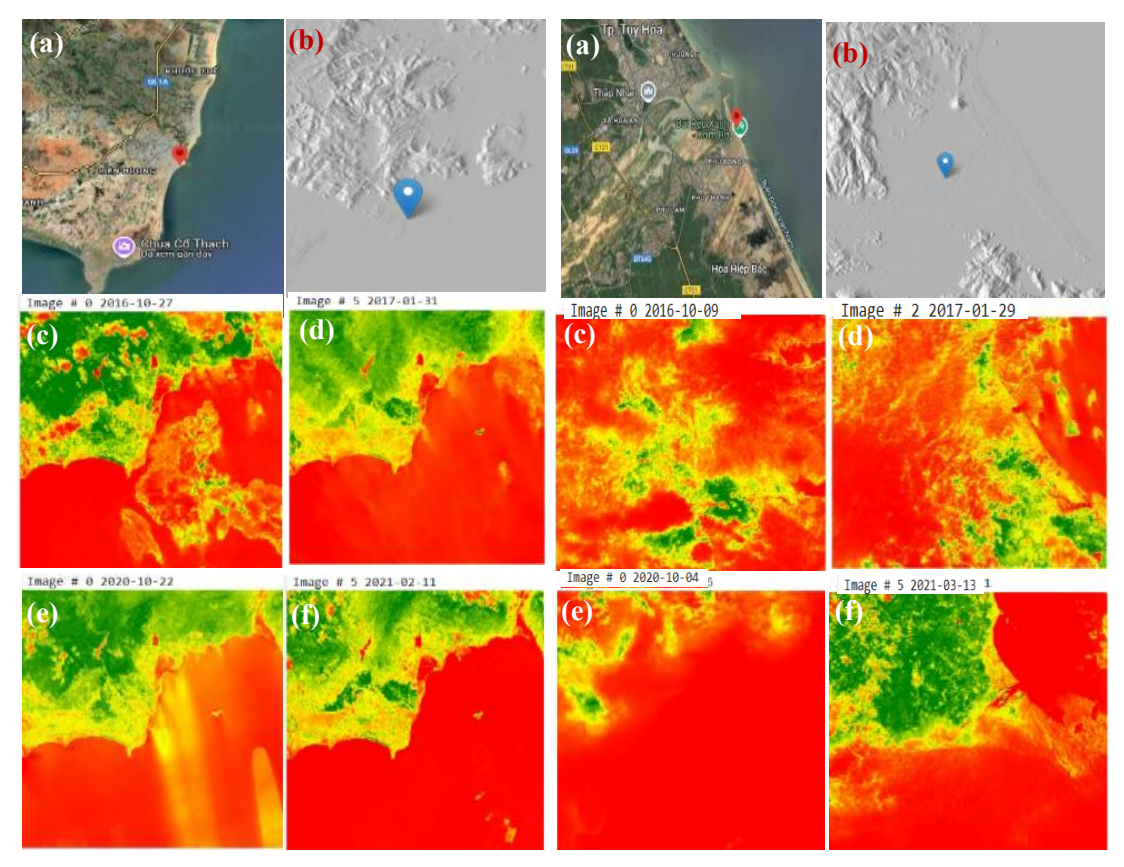


Figure 7. LienHuong's Shoreline Erosion during 2016 – 2021

Figure 8. Ro Hamlet's Shoreline Erosion during 2016 - 2021

Binh Thuan province: in Lien Huong Town, approximately 1,200 meters of coastline have been eroded, with land loss extending 50–100 meters inland. in addition, Figure 7 illustrates the progressive shoreline erosion in the town, over a five-year period using remote sensing and GIS techniques, and it reveals a gradual land retreat, with significant erosion observed along the shoreline and river mouth. Coastal vegetation degradation could be observed indicating enhanced susceptibility of wave action and sediment loss. This erosion is most likely due to natural coastal processes, upwelling of sea level rise because of climate change and human induced activities (aquaculture, sand mining).

Phu Yen Province: Erosion rate is 10 to below 20 meters/year in Ro Village, Tuy Hoa City has more erosion. With time this led to the loss of several to hundreds of hectares of land along rivers and coastal zones. Some of these, are aerial particularly hazardous containing ~248 km14 classified as Very High Risk. As more erratic weather patterns we see, coastal erosion visitation becomes more erratic in (local communes' anxiety counterbalancing) the authorities. Figure 8 also indicates a trend of shoreline retreat on much of the beach,

particularly in some large wave approach and tidal exposure areas. Decreasing coastal vegetation signifies erosion and sediment movement reach new dimensions.

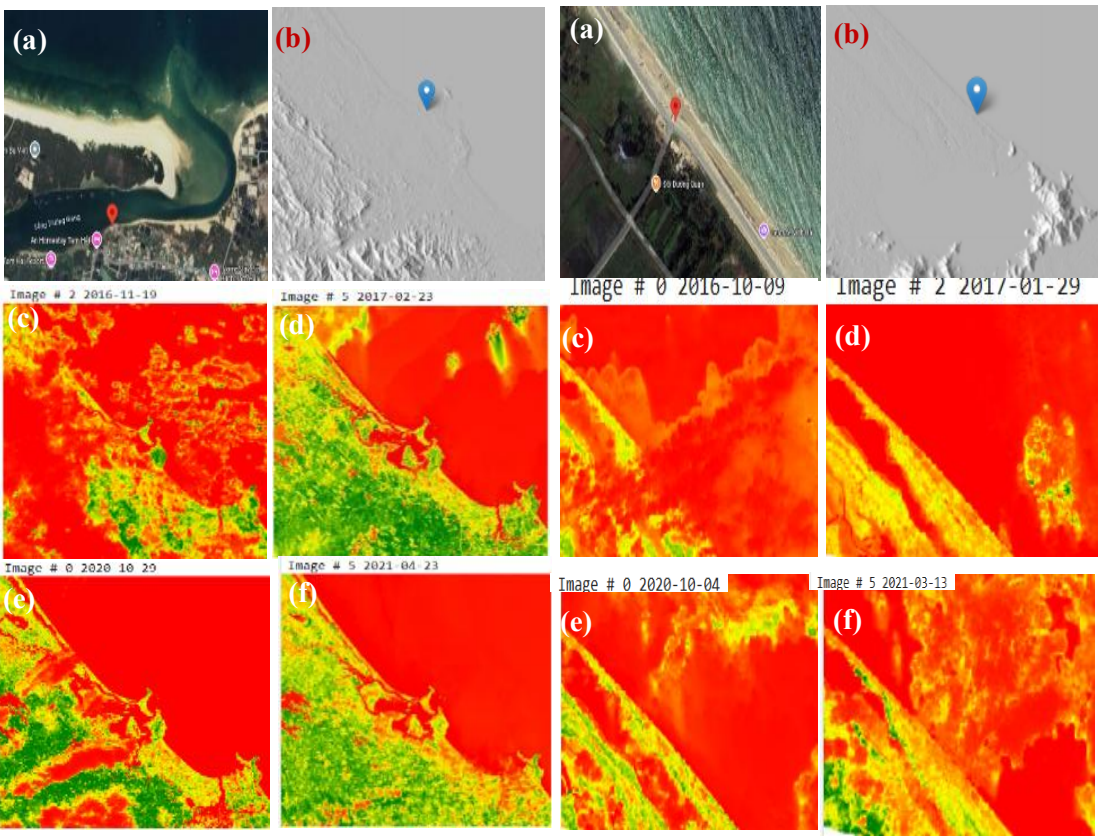


Figure 9. CuaLo Beach Erosion during 2016 - 2021

Figure 10. Giang Hai's Shoreline Erosion during 2016 - 2021

Quang Nam province: the CuaLo beach in Tam Hai Commune has seen substantial wave-induced erosion. Affected by waves, which have eroded seaward 3-5 meters and washed hundreds of Casuarina trees in a 2-kilometre stretch of coast in Binh Trung Hamlet Along with the temporary houses constructed for shrimp farming many old ponds are gone, and their graves. Also, shown in Figure 9 is an advanced land-loss along shallow nearshore areas, especially regions of high wave energy. The loss of vegetated zones implies a significant exposure to coastal erosion and sediment transport processes. This shoreline instability may be also exacerbated by other human activities in the form of large tourism development or infrastructure expansion.

Hue City: Sea erosion has caused loss of hundreds of hectares of trees, forests and farmlands along three seaside communes. The most extensive area had a loss of more than 150 hectares including 90 hectares of rice, crops and 60 hectares ponds and freshwater reservoirs for shrimp, crab, as well as fisheries in Giang Hai commune. In conjunction with Figure 10 which demonstrates the tidal influences, wave agitation and anthropological factors; A substantial decrease in vegetated area may have helped increase the erosion sensitivity.

Quang Tri Province: Sea dike has been entirely torn for more than 150 meters; waves breaching into the land and topple down local shop that threaten row of coastal infrastructure, in Vinh Thai Commune. Be along with, Figure 11 displays the erosion is particularly prominent along the eastern shoreline, where land degradation is noticeable. Factors contributing to this process include wave action, sea-level rise, extreme weather events, and anthropogenic activities. A reduction in coastal vegetation, particularly mangroves, may have further exposed the shoreline to erosion.

Kien Giang Province: In Tay Yen Commune, A Bien District, since last decade (2011–2023) the coastal erosion has intensified so about 500 hectares of mudflats lose each year. The coastal forest belt has retreated 60 to 300 meters, or approximately 20 m/year - 3 m/year degradation of coastal forest plantation. Currently erosion has affected approximately 188 kilometers, out of the province's 254 kilometers of coastline. Figure 12c and 12f detail data indicate a large extent of land loss in the coastal zone (red areas show up more prominent in the north and central parts). The erosion-dotted line of deposition at least hints at some environmental stresses which may increase over time through wave action, tidal and anthropogenic influence as well.

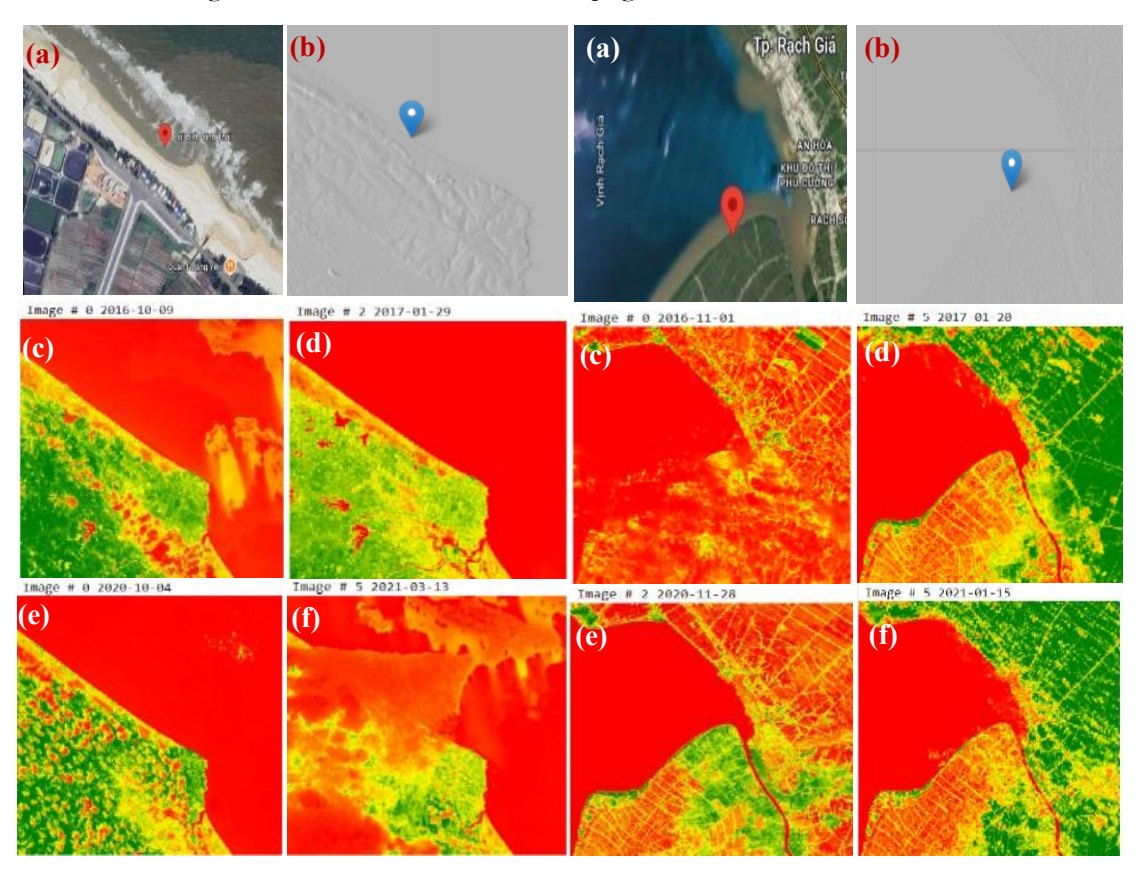


Figure 11. Vinh Thai's Shoreline Erosion during 2016-2021

Figure 12. Tay Yen Conmunm's Coastal Erosion during 2016-2021

Tra Vinh province: Hiep Thanh commune of the coastline received a lot of erosion from the blow of monsoon waves and high tides in Tra Vinh Province. Erosion has been highly intense (> 900 meters shoreline and 50 meters inland penetration) at some locations endangering 199 households. Figure 13c and Figure 13f outline the tremendous loss of land along the southern shoreline with the red areas encroaching into the land. The trend is manifested as ongoing coastal erosion possibly driven by wave action, sediment motion and human disturbances.

Ca Mau Province: Between 2011 and 2022, around 5,250 hectares of mangrove forests were lost due to coastal erosion. The worst-affected area, Tam Giang Tay, have suffered severe damage, directly impacting local livelihoods. Figure 14 describes a noticeable increase in red areas over time, and the northern section of the coastline appears to have undergone significant land loss. Possible causes include wave action, tidal currents, sediment transport, and human-induced activities such as aquaculture expansion. There is coastal vegetation, a lot mangroves especially reduced and be erosion speeded up.

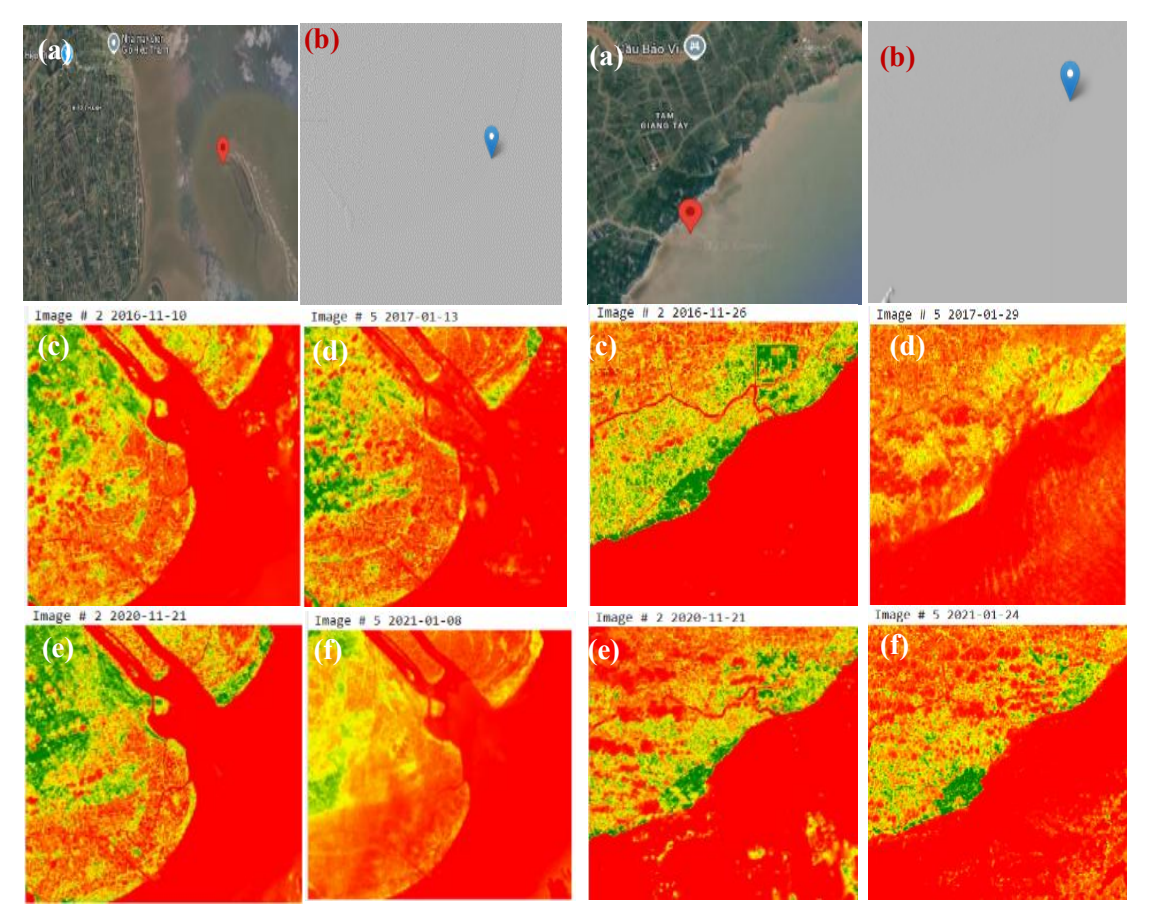


Figure 13. Hiep Thanh's Shoreline Erosion during 2016 – 2021

Figure 14. Tam Giang Tay's Shoreline Erosion during 2016 – 2021

Ben Tre Province: Approximately 4.7 km of Bao Thuan Commune, Ba Tri District have been eroded which impact directly to 115 households. Coastal erosion has eaten up 100 meters of concrete roads, some 650 meters embankments and more than 535 hectares land. 15 houses were damaged with 4 completely collapse and 11 families were relocated. Land loss along the southern shoreline is evident in Figure 15 and represents a very high rate of erosion from the coastline. Possible explanations are the wave action, tidal currents and sea-level rise and anthropogenic activities such as deforestation. Coastal vegetation loss coupled accelerates erosion and sediment displacement.

Bac Lieu: Erosion has taken protective forests away so the waves directly striking the dikes, in some parts. One of the most affected areas is the Ganh Hao. Moreover, Figure 16 depicts the shoreline changes to appear along the southern coastline, where land loss is more pronounced. Contributing factors include wave action, sediment transport, tidal forces, and possible anthropogenic impacts.

Coastal vegetation cover reduces, which could in turn promote erosion by sediments destabilizing. Vietnam faces an urgent environmental and socio-economic threat due to rapid coastal erosion. The elimination of protection forests, farmland and all-terrain infrastructure has grave implications for local communities and the economy. Much-needed quick and effective mitigation options are required to protect and preserve Vietnam coastline from development. From the above analysis, the main factors underlying coastal erosion in Vietnam are classified into natural factors and human-induced factors.

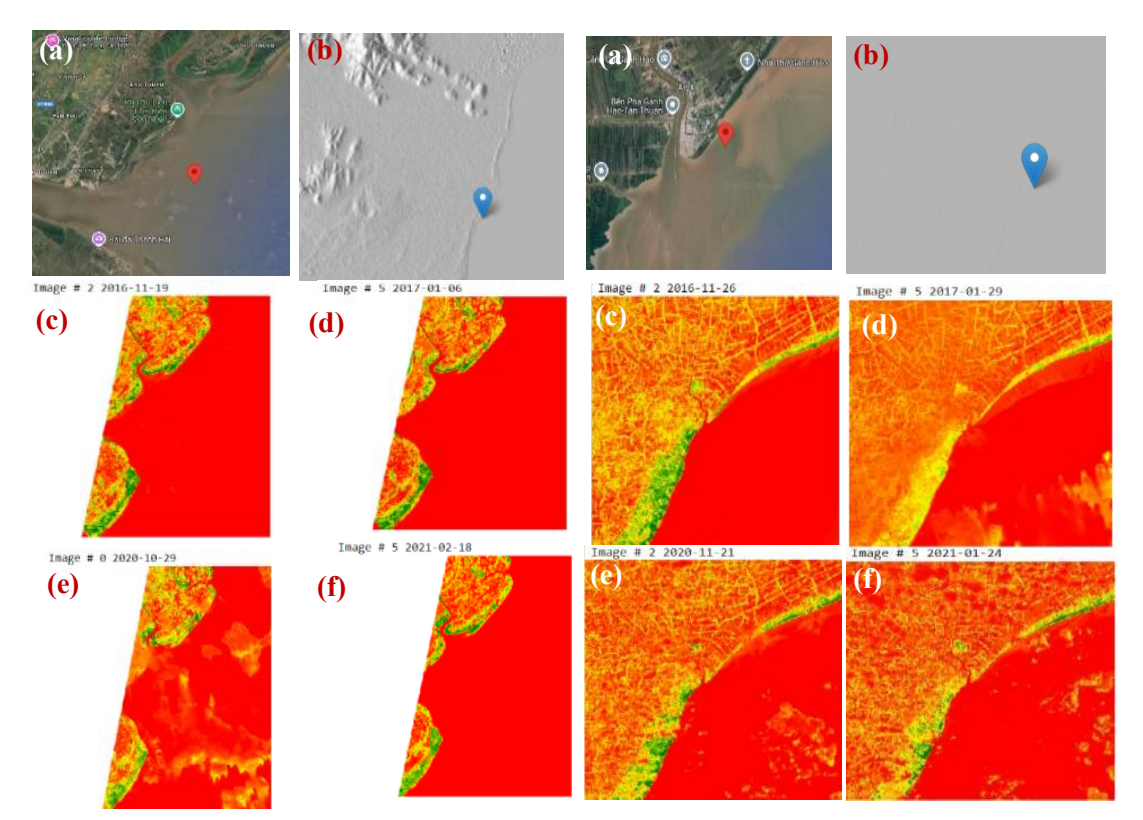


Figure 15. Bao Thuan's Shoreline Erosion during 2016 – 2021

Figure 16. GanhHao Shoreline Erosion during 2016-2021

The impacts of climate change on coastal erosion include; (1) Porosity of soil is essential for its water-uptake and -drainage Soil porosity, such as in poorly drained soil or compacted clay soils, restricts the infiltration of water (Nearing et al., 1989; Toy et al., 2002). High porosity soils like sand drain more freely. Sandy soils have high porosity, which encourage quick water entry Low Porosity, such as compacted clay low soil water-infiltration, can cause surface runoff and further erosion High-porosity soils, like sandy ones, increase water infiltration For example, this can help reduce surface erosion (Lal & Stewart, 2018; Shukla, 2003); (2) The high tides, mainly occurring during storm surges increase wave energy over coastal erosion including elevated tides exacerbated by storm surges (Komar, 1977; Masselink et al., 2014; Pugh, 2004). Variations in tidal level will also change the amount of shoreward march waves may attain onto the shore (Nicholls & Cazenave, 2010).

- (3) Monsoon winds stir up and move more sediment giving greater displacement in conjunction with faster shoreline retreat (Anthony et al., 2021; Masselink et al., 2014); (4) Persistent or heavy rainfall increase runoff, exacerbating the erosion of beaches and coastal cliffs. Turbulent runoff loosens soil structure, lower rain intensities (~100%) and thus make the coastal slopes prone to severe slope failures and associated sediment transport downstream to the ocean (Collins & Sitar, 2008; Crozier, 2010; Sidle & Bogaard, 2016); (5) Storm events significantly impact on coastal erosion. At the same time, the event surges elevate sea levels, facilitating the rapid movement of sediments and the degradation of coastal formations (Sallenger Jr, 2000; Zhang et al., 2004).
- (6) Coastal Geomorphology (shore face) gradient drives erosion rates; steeper slopes induce greater longshore sediment transport due to the force of gravity (Bird, 2008; Cowell & Thom, 2006). In contrast, more slowly eroding coastlines may deposit and accumulate sediments (Masselink et al., 2014); (7) Increased wave heights drive the most enhanced erosion due to wave forces on coastal landscapes (Komar, 1977; Masselink et al., 2014). Continuous wave action has an important influence in the horizontal re-suspension of sediments,

therefore moving materials up and over shore (Cowell & Thom, 2006); (8) Sea level rise slowly submerges the coastal areas and amplify chronic erosion. Higher sea levels will reach more inland- their waves can travel further (Church & White, 2011; Nicholls & Cazenave, 2010), and (9) Rising global temperatures expansion of ocean water is another thermal load that drives sea level rise. Even more frequent and severe storms and cyclones will further exacerbate coastal erosion (Hansen et al., 2013; Rahmstorf, 2007).

Anthropogenic influences on shoreline retreat consisting of deforestation of Protective Mangrove Forests: mangrove removal reduces natural defenses against erosion (Duke et al., 2007; Giri et al., 2011); coastal Engineering and Development: Poorly planned construction of walls and dikes change the sediment flow, thereby exacerbating erosion (Anthony, 2016; Hapke et al., 2009); aquaculture/land use changes (excessive shrimp farming and conversion of land forces it to destabilize; amount of fishermen reported washed away land-based extraction (Barbier et al., 2013; Hamilton, 2013; Primavera, 2006).

Vietnam continental type coastline degradation is brought about by a complex mixture of climatic, oceanic, geological and also anthropogenic activities. To cope with this, integrated coastal zone management (book cover report perhaps) is vital which includes restoration of mangrove systems, livelihood regulation and also construction coastal security to reduce damages further.



Figure 17. Coastal Erosion Points

The data for this study was sourced from the Open Development Mekong website, the National Centre for Hydro-Meteorological Forecasting of Vietnam, and Landsat 8 OLI/TIRS satellite imagery for six years (from 2016 to 2022). Using Python, an analysis was conducted on 52 coastal erosion sites along the Vietnamese shoreline; at the same time, 52 gathered samplers are divided into 80%, and 20% for training and testing phases. Figure 17 demonstrates the locations of beach erosion, categorized by severity levels: Level 5 ("Hazardous points without planned repair funding") – Red, Level 4 ("Hazardous points with planned repair funding") – Orange, Level 3 ("Extremely hazardous points") – Green, Level 2 ("Normal erosion points") – Blue, Level 1 ("Points with extremely critical erosion velocity") – Purple. Natural negative factors affecting coastal erosion: Tide height (m), wave height (m), storm intensity (km/h), storm geomorphology slope(degree), monsoon winds (km/h), rainfall (l), sea level rise (m), temperature (°c).

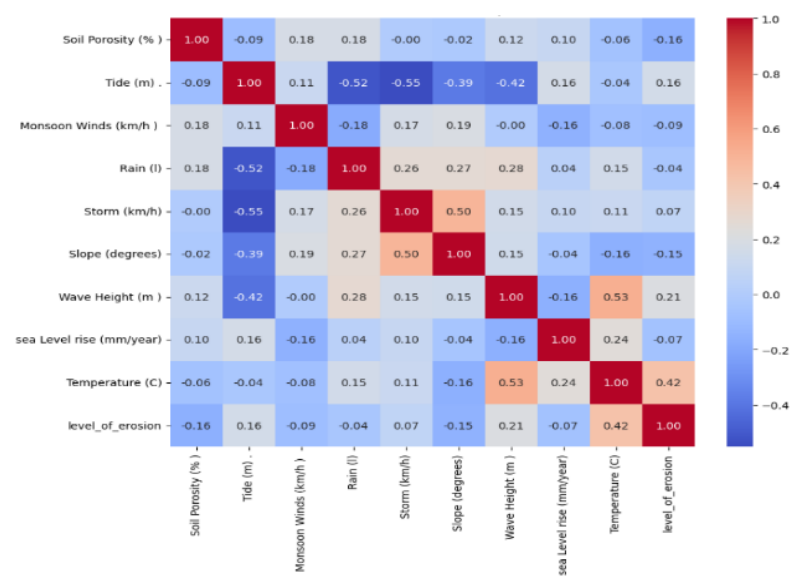


Figure 18. Pearson Correlation Matrix for Coastal Erosion Factors

For all things except coastal geomorphology the scale of these forces was mapped by their equal annual, average measured. Figure 18 explains the distribution of variables based on Pearson correlation coefficients, which quantify the strength and direction of their relationships. These coefficients range from -1 to 1 (Asuero et al., 2006; Šverko et al., 2022), where higher absolute values indicate stronger associations, while values closer to 0 suggest weaker correlations. The Pearson correlation analysis revealed varying degrees of association among key environmental factors, with certain variables exhibiting strong positive correlations. Contrarily another could have weak or even negative associations. Specifically, the analysis also identified positive relationships including coastal geomorphology and storm intensity (CC = 0.50) with temperature (CC = 0.53), wave height. In contrast, tidal height showed negative correlations with rainfall (-0.52), storm intensity (-0.55), coastal slope (-0.39), and wave height (-0.42). Sea Level Erosion also upon closer observation showed minor positive correlation with temperature (CC = 0.42).

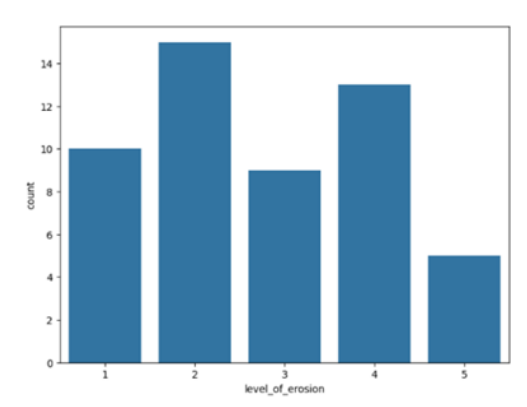


Figure 19. Statistic for Level of Coastal Erosion

Table 1 illustrates some descriptive statistics of MEAN, standard deviation (STD), minimum (Min), maximum(Max) parameters of data quality across 42 stations, Moreover MEAN and STD of input evaluator attributes are soil porosity(38.27,6.33), tide height (2.48,0.64), monsoon winds (43.37,8.67), rainfall (2.33,0.44), storm intensity (151.35,34.47), coastal slope (4.40,4.12), wave height(1.92,0.88), sea level rise (4.81,0.53), temperature (30.21,1.09), the level of erosion (2.77,1.29). The STD range is concentrated near the MEAN with minimal variation, indicating acceptable reliability for forecasting coastal erosion changes. In addition, Figure 19 displays the levels of coastal erosion, indicating that along the Vietnamese shoreline, Level 1, Level 2, Level 3, Level 4, and Level 5 correspond to 10, 15, 9, 13, and 5 points, respectively.

Tidal Rainf Storm Coastal Wave Cate Soil Monsoon Sea level rise Tempera Level of all (l) porosity height intensity height gory winds slope (mm/year) ture (o^c) erosion (m) (%) (m) (km/h) (km/h) (degree) MEAN 38.27 43.37 2.33 151.35 1.92 30.21 2.77 2.48 4.40 4.811.29 STD 6.33 0.64 8.67 0.44 34.47 4.12 0.88 0.531.09 MIN 25 2 25 1.2 80 1 1 3 271 MAX 60 4 70 3.5 200 20 4 5 32 5

Table 1. Descriptive Data Analysis

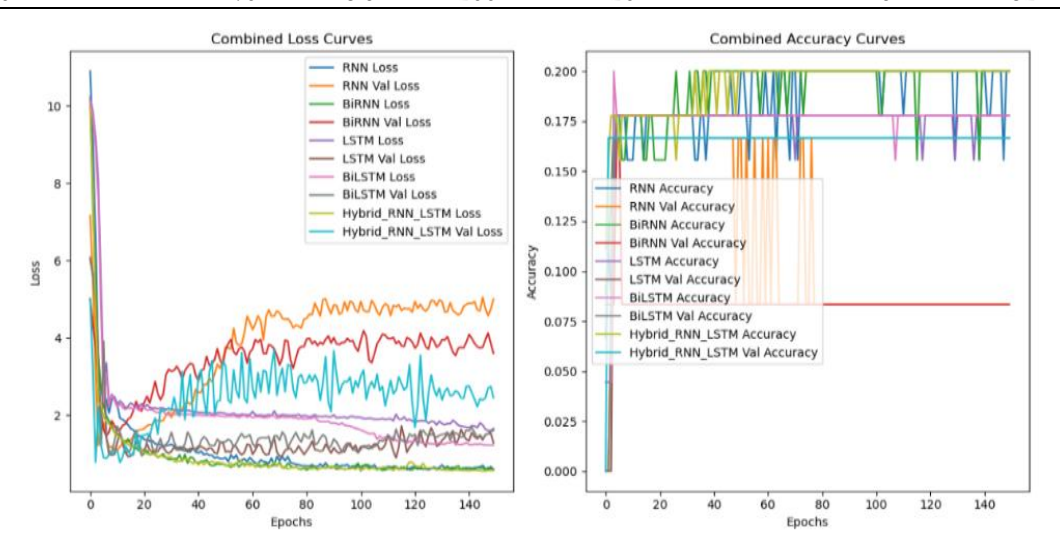


Figure 20. (a) Training Loss, (b) Validation Loss for Activation Functions using 5 Models

Regarding to deploy deep learning for coastal erosion analysis, Figure 20 presents the combined loss curves (loss and validation loss) and accuracy curves (accuracy and validation accuracy) for the five models at the 150th epoch. The diagrams highlight the influence of convergence and model performance, revealing that the validation loss and accuracy of the RNN and its variant models failed to converge. Meanwhile, other models exhibited significant fluctuations under specific training conditions, indicating instability in their learning process. Additionally, the study conducted experiments on all models, and the results presented in Table 2, and Figure 21 present the simulation outcomes of the five models. Results suggest the best forecasting model is Hybrid RNN_LSTM (5.85) followed by simple RNN. The other models (LSTM, BiRNN, BiLSTM) also provide reasonable performance but somewhat lower in accuracy than the top two models.

Model **RMSE** R_squared MAE CC STD RNN 0.77 0.740.430.90 1.62 BiRNN 0.93 0.530.570.861.80 LSTM 0.83 0.66 0.770.850.61 BiLSTM 0.88 0.51 0.740.80 0.84 Hybrid RNN_LSTM 0.710.77 0.35 0.91 1.54

Table 2. Standard Metrics for Accuracy

A Taylor diagram illustrates in a graphical way how STD and CC are related for varying models (RNNs, BiRNNs, LSTMs and Bi-LSTMs and Hybrid_RNN_LSTM) against an ideal reference. In particular, Figure 22 shows a visual STD and CC comparisons for STD from different models. The Hybrid RNN-LSTM model has strongest correlation (0.91) with smallest standard deviation; hence, this is considered as a perfect forecasting model. The RNN model showed good performance with CC of ~0.90. Other models (BiRNN, LSTM, BiLSTM) have relatively lower CC values.

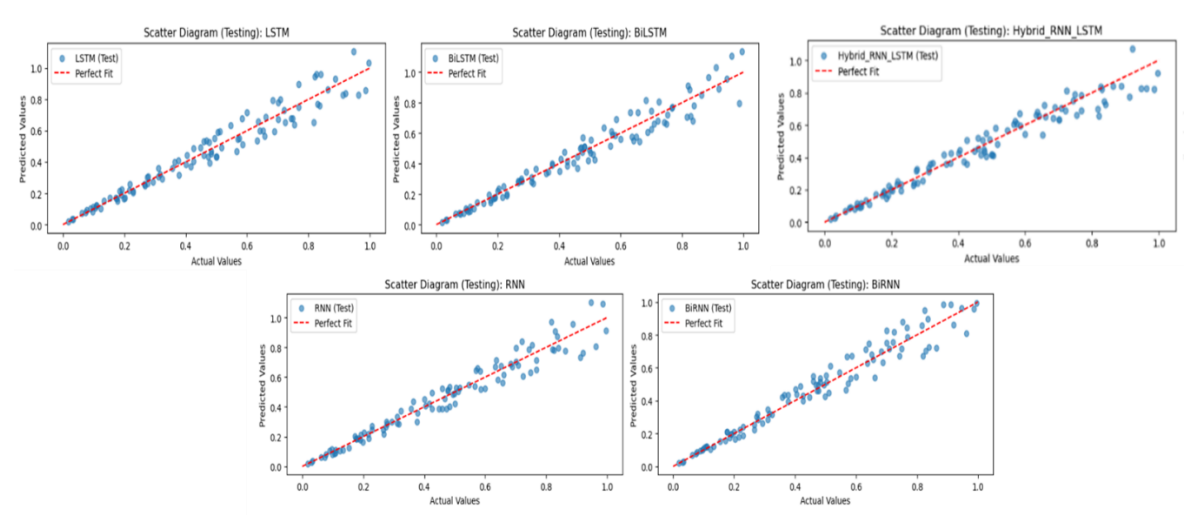


Figure 21. The Regression for Forecasting of Five Models based on Testing Phase

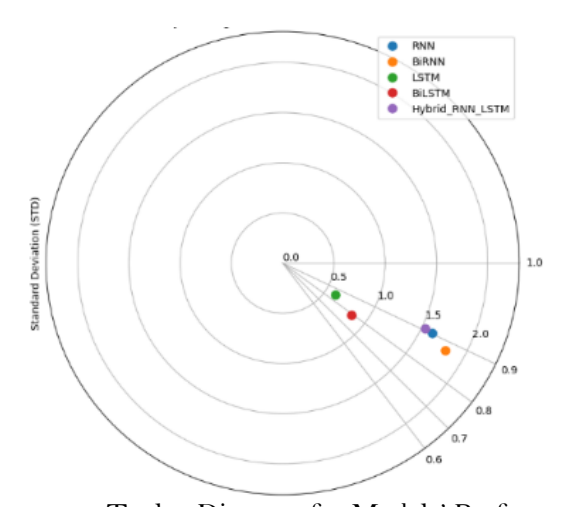


Figure 22. Taylor Diagram for Models' Performance

Figure 23 summaries SHAP plot to provide insights into the impact of different features on the model's predictions for coastal erosion levels. It highlights that Monsoon Winds, Storm Intensity, and Tidal Height have the most significant influence, as indicated by the wider spread of SHAP values along the x-axis. These combination of features have a positive contribution as well as a negative one, meaning that they play an important role on differences in coastal erosion. They influence the model, too: Coastal Slope, Wave Height and Soil Porosity have a lower SHAP value where, again the range is smaller than Monsoon Winds or Tidal Height but higher than more moderate impacts in contrast Sea Level Rise and Rainfall display less SHAP values spread suggesting a lesser overall effect.

On the other hand, sea level rise and Rainfall have not such rounded SHAP values span (smaller effect), as an example. Rainfall appears to have almost zero effect, with SHAP values distributed around zero which would mean minor influence on the model. Image the northern coast to southern regions of Vietnam: One of the countries which gets maximum tempo changed weather, Coastal erosion has been the most threatening issue on land from northwards. Studying and predicting coastal erosion is therefore central to developing effective mitigation strategies for local communities to help reduce its impact. We used the forecasting models to predict coastal erosion at 52 sites along Vietnam coastline, this study findings showed that the number of erosion points is highest in Mekong Delta, followed by Central Coast and Red River Delta. Recent (2010 and later) Landsat 8 OLI/TIRS satellite imagery analysis revealed that these are treeless regions and predominantly located at the

mouths, where high sediment transport potentially balances coastal resilience across this extent. This study was based on nine main natural factors for coastal erosion as major drivers. While the model can be more precise if additional parameters such as human activities were considered, the deep learning-based approach offers accurate forecasting features. The conclusion of this research indicated that the five predictive models are good predicting models and effective for forecasting study canyon landslides in regions with specific environmental condition.

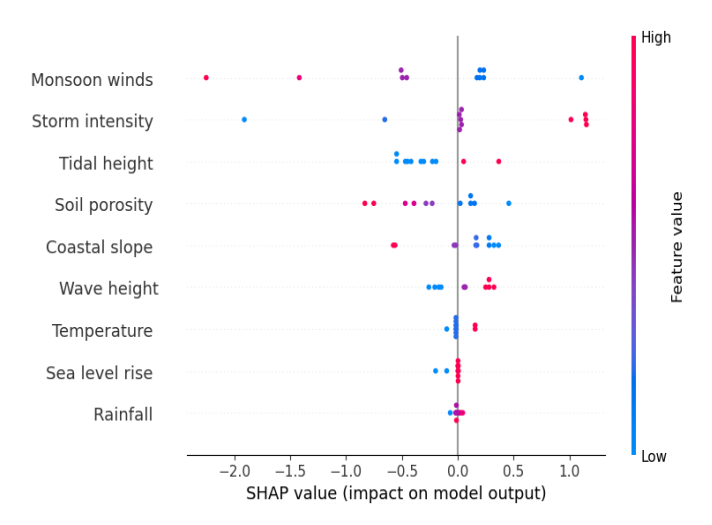


Figure 23. The Impact of Different Features on the Model's Predictions for Coastal Erosion Levels

4. Conclusion

Vietnamese coastline is a pretty valuable natural capital with its mesmerizing views, marvelous biodiversity and huge economic value. Nevertheless, it is currently more and more being injured naturally but also by human activities. People need to ensure sustainable development and conservation programs in order to preserve this key in next generations' use. Developed deep learning models to evaluate and predict coastal erosion along Vietnam's coastline by combining nine mandatory registers of the surrounding environmental conditions of this study. The results showed that the Hybrid RNN_LSTM model outperformed other models in terms of accuracy and reliability. Some of the most important were monsoon winds, storm power, tidal height, whereas, rainfall and sea level rise only had a small effect on erosion prediction.

The main consideration of this study was focused on nine input factors but with consideration of other impacting elements like impact of human intervention, subsurface sedimentogenics and ocean currents. These findings recommend a robust foundation for integrating deep learning into coastal management frameworks, offering actionable insights for climate adaptation strategies. Furthermore, the analysis is based on only five predictive models which arguably might open an opportunity for improved performance without exploring the effect of other models such as Hybrid BiRNN_LSTM and BiRNN_BiLSTM.

5. Acknowledgement

Thanks for group research number of NCTB.DHH.2024.05 of Hue University.

6. References

Al-Selwi, S. M., Hassan, M. F., Abdulkadir, S. J., Muneer, A., Sumiea, E. H., Alqushaibi, A., & Ragab, M. G. (2024). RNN-LSTM: From Applications to Modeling Techniques and Beyond—Systematic Review. *Journal of King Saud University-Computer and Information Sciences*, 36(5), 102068. [Crossref]

Anthony, E. J. (2016). Assessment of Peri-Urban Coastal Protection Options in Paramaribo-Wanica, Suriname. In WWF Guianas, Paramaribo, Suriname.

Anthony, E. J., Gardel, A., Zainescu, F., & Brunier, G. (2021). Fine sediment systems. Reference Module in Earth Systems and Environmental Sciences, 1016, 130–139. [Crossref]

- Asuero, A. G., Sayago, A., & González, A. G. (2006). The Correlation Coefficient: an Overview. *Critical Reviews in Analytical Chemistry*, 36(1), 41–59. [Crossref]
- Barbier, E. B., Georgiou, I. Y., Enchelmeyer, B., & Reed, D. J. (2013). The Value of Wetlands in Protecting Southeast Louisiana from Hurricane Storm Surges. *PLOS ONE*, 8(3), e58715. [Crossref]
- Bird, E. C. F. (2008). Coastal Geomorphology: an Introduction. John Wiley \& Sons.
- Brocx, M., & Semeniuk, V. (2009). Coastal Geoheritage: Encompassing Physical, Chemical, and Biological Processes, Landforms, and Other Geological Features in the Coastal Zone. *Journal of the Royal Society of Western Australia*, 92, 243–260.
- Brown, J. B. (2018). Classifiers and their Metrics Quantified. Molecular Informatics, 37(1-2), 1700127. [Crossref]
- Church, J. A., & White, N. J. (2011). Sea-level rise from the late 19th to the early 21st century. Surveys in Geophysics, 32(4), 585-602. [Crossref]
- Collins, B. D., & Sitar, N. (2008). Processes of Coastal Bluff Erosion in Weakly Lithified Sands, Pacifica, California, USA. Geomorphology, 97(3–4), 483–501. [Crossref]
- Cowell, P. J., & Thom, B. G. (2006). Discussion of: . Management of Uncertainty in Predicting Climate-Change Impacts on Beaches. *Journal of Coastal Research*, 22(6), 1577–1579. [Crossref]
- Crozier, M. J. (2010). Deciphering the Effect of Climate Change on Landslide Activity: A Review. Geomorphology, 124(3-4), 260-267. [Crossref]
- Dong, W. S., Ismailluddin, A., Yun, L. S., Ariffin, E. H., Saengsupavanich, C., Maulud, K. N. A., Ramli, M. Z., Miskon, M. F., Jeofry, M. H., Mohamed, J., & others. (2024). The Impact of Climate Change on Coastal Erosion in Southeast Asia and the Compelling Need to Establish Robust Adaptation Strategies. *Heliyon*, 10(4). [Crossref]
- Donkol, A. A. E.-B., Hafez, A. G., Hussein, A. I., & Mabrook, M. M. (2023). Optimization of Intrusion Detection using Likely Point PSO and Enhanced LSTM-RNN Hybrid Technique in Communication Networks. *IEEE Access*, 11, 9469–9482. [Crossref]
- Duc, D. M., & Hieu, N. M. (2017). Analysis of Sea-Level Rise Impacts on Sea Dike Stability in Hai Hau Coast, Vietnam. *International Journal of Civil Engineering*, 15(3), 377–389. [Crossref]
- Duke, N. C., Meynecke, J.-O., Dittmann, S., Ellison, A. M., Anger, K., Berger, U., Cannicci, S., Diele, K., Ewel, K. C., Field, C. D., & others. (2007). A World without Mangroves? *Science*, 317(5834), 41–42. [Crossref]
- FitzGerald, D. M., Fenster, M. S., Argow, B. A., & Buynevich, I. V. (2008). Coastal Impacts ue to Sea-Level Rise. *Annu. Rev. Earth Planet. Sci.*, 36(1), 601–647. [Crossref]
- Gao, J. (2024). R-Squared (R2)--How much Variation is Explained? Research Methods in Medicine \& Health Sciences, 5(4), 104–109. \[\capprox \capprox \copyrightarrow \copyrightarrow \]
- Giri, C., Ochieng, E., Tieszen, L. L., Zhu, Z., Singh, A., Loveland, T., Masek, J., & Duke, N. (2011). Status and Distribution of Mangrove Forests of the World using Earth Observation Satellite Data. *Global Ecology and Biogeography*, 20(1), 154–159. [Crossref]
- Gracia, A., Rangel-Buitrago, N., Oakley, J. A., & Williams, A. T. (2018). Use of Ecosystems in Coastal Erosion Management. Ocean & Coastal Management, 156, 277–289. [Crossref]
- Hameed, Z., & Garcia-Zapirain, B. (2020). Sentiment Classification using a Single-Layered BiLSTM Model. *Ieee Access*, 8, 73992–74001. [Crossref]
- Hamilton, S. (2013). Assessing the Role of Commercial Aquaculture in Displacing Mangrove Forest. *Bulletin of Marine Science*, 89(2), 585–601. [Crossref]
- Hansen, J., Sato, M., Russell, G., & Kharecha, P. (2013). Climate Sensitivity, Sea Level and Atmospheric Carbon Dioxide. *Philosophical Transactions of the Royal Society A: Mathematical, Physical and Engineering Sciences*, 371(2001), 20120294. [Crossref]
- Hapke, C. J., Reid, D., & Richmond, B. (2009). Rates and Trends of Coastal Change in California and the Regional Behavior of the Beach and Cliff System. *Journal of Coastal Research*, 25(3), 603–615. [Crossref]
- Hens, L., Thinh, N. A., Hanh, T. H., Cuong, N. S., Lan, T. D., Van Thanh, N., & Le, D. T. (2018). Sea-Level Rise and Resilience in Vietnam and the Asia-Pacific: A Synthesis. *Vietnam Journal of Earth Sciences*, 40(2), 126–152. [Crossref] Karch, J. (2020). Improving on Adjusted R-Squared. *Collabra: Psychology*, 6(1), 45. [Crossref]
- Kardani, N., Zhou, A., Nazem, M., & Shen, S.-L. (2020). Estimation of Bearing Capacity of Piles in Cohesionless Soil using Optimised Machine Learning Approaches. *Geotechnical and Geological Engineering*, 38(2), 2271–2291. [Crossref]
- Karlsrud, K., Vangelsten, B. V, & Frauenfelder, R. (2017). Subsidence and Shoreline Retreat in the Ca Mau Province—Vietnam: Causes, Consequences and Mitigation Options. *Geotechnical Engineering Journal of the SEAGS & AGSSEA*, 48(1), 26–32. [Crossref]
- Kim, S., & Kim, H. (2016). A New Metric of Absolute Percentage Error for Intermittent Demand Forecasts. *International Journal of Forecasting*, 32(3), 669–679. [Crossref]
- Komar, P. D. (1977). Beach Processes and Sedimentation.
- Lal, R., & Stewart, B. A. (2018). Soil and Climate. CRC Press, Taylor & Francis Group.

- Li, Q., Ness, P. M., Ragni, A., & Gales, M. J. F. (2019). Bi-Directional Lattice Recurrent Neural Networks for Confidence Estimation. ICASSP 2019-2019 IEEE International Conference on Acoustics, Speech and Signal Processing (ICASSP), 6755-6759. [Crossref]
- Lin, T. Y., Van Onselen, V. M., & Vo, L. P. (2021). Coastal Erosion in Vietnam: Case studies and Implication for Integrated Coastal Zone Management in the Vietnamese South-Central Coastline. *IOP Conference Series: Earth and Environmental Science*, 652(1), 12009. [Crossref]
- Lindemann, B., Müller, T., Vietz, H., Jazdi, N., & Weyrich, M. (2021). A Survey on Long Short-Term Memory Networks for Time Series Prediction. *Procedia Cirp*, 99, 650–655. [Crossref]
- Liu, D. Z., & Singh, G. (2016). A Recurrent Neural Network based Recommendation S ystem. International Conference on Recent Trends in Engineering, Science & Technology.
- Masselink, G., Hughes, M., & Knight, J. (2014). Introduction to Coastal Processes and Geomorphology. Routledge. [Crossref]
- Ming, Y., Cao, S., Zhang, R., Li, Z., Chen, Y., Song, Y., & Qu, H. (2017). Understanding Hidden Memories of Recurrent Neural Networks. 2017 IEEE Conference on Visual Analytics Science and Technology (VAST), 13-24. [Crossref]
- Morton, R. A. (2003). An Overview of Coastal Land Loss: with Emphasis on the Southeastern United States. US Geological Survey, Center for Coastal and Watershed Studies St~....
- Nearing, M. A., Foster, G. R., Lane, L. J., & Finkner, S. C. (1989). A Process-based Soil Erosion Model for USDA-Water Erosion Prediction Project Technology. *Transactions of the ASAE*, 32(5), 1587–1593. [Crossref]
- Nga, T. N. Q., Bay, N. T., Long, T. T., & Hoai, H. C. (2025). Drivers and Mechanisms of Erosion in the Vietnamese Mekong Delta. In *The Mekong Delta Environmental Research Guidebook* (pp. 107–130). Elsevier. [Crossref]
- Nguyen, A. T., Vu, A. D., Dang, G. T. H., Hoang, A. H., & Hens, L. (2018). How do Local Communities Adapt to Climate Changes along Heavily Damaged coasts? A Stakeholder Delphi Study in Ky Anh (Central Vietnam). *Environment, Development and Sustainability*, 20(2), 749–767. [Crossref]
- Nicholls, R. J., & Cazenave, A. (2010). Sea-Level Rise and Its Impact on Coastal Zones. *Science*, 328(5985), 1517–1520. [Crossref]
- Nichols, C. R., Zinnert, J., & Young, D. R. (2018). Degradation of Coastal Ecosystems: Causes, Impacts and Mitigation Efforts. In *Tomorrow's Coasts: Complex and Impermanent* (pp. 119–136). Springer. [Crossref]
- Niedbała, G. (2019). Simple Model based on Artificial Neural Network for Early Prediction and Simulation Winter Rapeseed Yield. *Journal of Integrative Agriculture*, 18(1), 54–61. [Crossref]
- Owens, P. N. (2020). Soil Erosion and Sediment Dynamics in the Anthropocene: A Review of Human Impacts during a Period of Rapid Global Environmental Change. *Journal of Soils and Sediments*, 20(12), 4115-4143. [Crossref]
- Primavera, J. H. (2006). Overcoming the Impacts of Aquaculture on the Coastal Zone. Ocean & Coastal Management, 49(9–10), 531–545. [Crossref]
- Pugh, D. (2004). Changing Sea Levels: Effects of Tides, Weather and Climate. Cambridge University Press.
- Rahmstorf, S. (2007). A Semi-Empirical Approach to Projecting Future Sea-Level Rise. *Science*, 315(5810), 368–370. [Crossref]
- Sahavacharin, A., Sompongchaiyakul, P., & Thaitakoo, D. (2022). The Effects of Land-based Change on Coastal Ecosystems. Landscape and Ecological Engineering, 18(3), 351–366.
- Salih, A. A., & Abdulazeez, A. M. (2021). Evaluation of Classification Algorithms for Intrusion Detection System: A Review. *Journal of Soft Computing and Data Mining*, 2(1), 31–40. [Crossref]
- Sallenger Jr, A. H. (2000). Storm Impact Scale for Barrier Islands. *Journal of Coastal Research*, 16(3), 890–895. [Crossref] Shukla, M. K. (2003). *Soil Physics: An Introduction*. CRC Press, Taylor & Francis Group. [Crossref]
- Siami-Namini, S., Tavakoli, N., & Namin, A. S. (2019). The Performance of LSTM and BiLSTM in Forecasting Time Series. 2019 IEEE International Conference on Big Data (Big Data), 3285–3292. [Crossref]
- Sidle, R. C., & Bogaard, T. A. (2016). Dynamic Earth System and Ecological Controls of Rainfall-Initiated Landslides. *Earth-Science Reviews*, 159, 275–291. [Crossref]
- Šverko, Z., Vrankić, M., Vlahinić, S., & Rogelj, P. (2022). Complex Pearson correlation Coefficient for EEG Connectivity Analysis. *Sensors*, 22(4), 1477. [Crossref]
- Thepsiriamnuay, H., & Pumijumnong, N. (2019). Modelling Assessment of Sandy Beaches Erosion in Thailand. *Environment and Natural Resources Journal*, 17(2), 71–86. [Crossref]
- Touzani, S., Granderson, J., & Fernandes, S. (2018). Gradient Boosting Machine for Modeling the Energy Consumption of Commercial Buildings. *Energy and Buildings*, 158, 1533–1543. [Crossref]
- Toy, T. J., Foster, G. R., & Renard, K. G. (2002). Soil Erosion: Processes, Prediction, Measurement, and Control. John Wiley & Sons, Inc.
- Van Tho, N. (2019). Coastal Erosion, River Bank Erosion and Landslides in the Mekong Delta: Causes, effects and Solutions. Geotechnics for Sustainable Infrastructure Development, 957–962. [Crossref]
- Veettil, B. K., Ward, R. D., Dung, N. T. K., Van, D. D., Quang, N. X., Hoai, P. N., & Hoang, N.-D. (2021). The Use of Bioshields for Coastal Protection in Vietnam: Current Status and Potential. Regional Studies in Marine Science, 47, 101945. [Crossref]

- Weerakody, P. B., Wong, K. W., Wang, G., & Ela, W. (2021). A Review of Irregular Time Series Data Handling with Gated Recurrent Neural Networks. *Neurocomputing*, 441, 161–178. [Crossref]
- Xiang, Z., Yan, J., & Demir, I. (2020). A Rainfall-Runoff Model With LSTM-Based Sequence-to-Sequence Learning. Water Resources Research, 56(1), e2019WR025326. [Crossref]
- Yaacob, R., Shaari, H., Sapon, N., Ahmad, M. F., Arifin, E. H., Zakariya, R., & Hussain, M. L. (2018). Annual Changes of Beach Profile and Nearshore Sediment Distribution Off Dungun-Kemaman, Terengganu, Malaysia. *Jurnal Teknologi* (Sciences & Engineering), 80(5). [Crossref]
- Yasuhara, K., Tamura, M., Van, T. C., & Duc, D. M. (2016). Geotechnical Adaptation to the Vietnamese Coastal and Riverine Erosion in the Context of Climate Change. Geotechnical Engineering Journal of the SEAGS & AGSSEA, 47(1), 7–14. [Crossref]
- Zhang, K., Douglas, B. C., & Leatherman, S. P. (2004). Global Warming and Coastal Erosion. *Climatic Change*, 64(1), 41–58. [Crossref]